Interactions of the QacR Multidrug-Binding Protein with Structurally Diverse Ligands: Implications for the Evolution of the Binding Pocket†

Steve Grkovic,‡ Kate M. Hardie, Melissa H. Brown, and Ronald A. Skurray*

School of Biological Sciences, University of Sydney, Sydney, New South Wales 2006, Australia

Received August 13, 2003; Revised Manuscript Received October 28, 2003

ABSTRACT: The QacR multidrug-binding repressor protein regulates the expression of the *Staphylococcus aureus qacA* gene, a multidrug resistance (MDR) locus that is prevalent in clinical isolates of this important human pathogen. In this paper we demonstrate that the range of structurally diverse compounds capable of inducing *qacA* transcription is significantly more varied than previously appreciated, particularly in relation to bivalent cations. For all of the newly identified inducing compounds, induction of *qacA* expression was correlated with a matching ability to dissociate QacR from operator DNA. Development of a ligand-binding assay based on intrinsic tryptophan fluorescence permitted dissociation constants to be determined for the majority of known QacR ligands, with values ranging from 0.2 to 82 μM. High-affinity binding of a compound to QacR in vitro was not found to correlate very strongly with either its in vivo inducing abilities or its structure. The latter observation indicated that the QacR ligand-binding pocket appears to have evolved to accommodate a wide range of toxic hydrophobic cations, rather than a specific class of compound. Importantly, the antimicrobial ligands of QacR included several plant alkaloids that share structural similarities with synthetic MDR substrates. This is consistent with the suggestion that the *qacA*−*qacR* MDR locus was recently derived from genes that protect against natural antimicrobial compounds.

Multidrug resistance (MDR)[1] transport proteins possessed by infectious microorganisms have emerged as a significant medical threat due to their impressive substrate ranges, which can include many antibiotics, antifungal agents, disinfectants, and antiseptics (*1*−*3*). Additionally, overexpression of the human MDR transporter, P-glycoprotein, in tumor cells can provide resistance to chemotherapeutic compounds (*4*). Although MDR transporters share the common property of mediating the export of structurally diverse toxic substrates, a large body of evidence suggests that for the majority of such pumps this function is not their intended physiological role, which is particularly apparent when it is taken into consideration that the majority of known MDR transporter substrates are synthetic compounds (*1*).

To assist efforts aimed at overcoming the health threats posed by the existence of MDR transporters, a number of important questions need to be addressed in relation to their function, such as determining the basis for their broad substrate range and the physiological functions of these proteins. The recently determined crystal structure of the MDR transport protein AcrB complexed to four different substrates has provided us with clues as to the mechanism employed by these proteins to recognize a range of compounds (*5*). Additionally, significant progress toward understanding the structural basis for multidrug recognition has been achieved via the analysis of soluble multidrug-sensing bacterial regulatory proteins, which mediate the expression of MDR genes via mechanisms that involve binding to a similar range of compounds as their cognate transporters (*6*, *7*). The publication of high-resolution structural data for the *Staphylococcus aureus* QacR repressor bound to each of six structurally diverse ligands (*8*) has provided us with a comprehensive view of the architecture of a multidrug-binding pocket, building upon earlier work which generated a structure for the *Bacillus subtilis* BmrR multidrug-binding regulator bound to a single ligand (*9*). The basis of multidrug binding revealed by these combined structures is the availability of a range of amino acid side chains lining the binding pocket that provide possibilities for the formation of alternative complementary electrostatic, aromatic stacking, and hydrophobic interactions with each ligand, assisted by opportunities for hydrogen bond formation.

Attempts to answer the second of the above questions has led to the identification of natural substrates for several MDR transporters (*7*, *10*−*14*). Although this represents an important first step, it must also be established whether the regulatory mechanisms governing the expression of the exporter in question mediate increased transporter production in response to the presence of these "physiological" substrates. Thus, the analysis of bacterial multidrug-sensing regulatory proteins can also help to determine whether the export of a natural compound represents a primary physiological role of a drug pump. However, the provision of

† This work was supported in part by Project Grants 153817 and 153818 from the National Health and Medical Research Council (Australia) to R.A.S. and M.H.B.

* To whom correspondence should be addressed. Tel: 61-2-9351-2376. Fax: 61-2-9351-4771. E-mail: skurray@bio.usyd.edu.au.

‡ Present address: INSERM U412, Ecole Normale Supérieure de Lyon, 46 allée d'Italie, 69364 Lyon Cedex 07, France.

[1] Abbreviations: MDR, multidrug resistance; P_{qacA}, *qacA* promoter; DAPI, 4′,6-diamidino-2-phenylindole; $DiOC_3$, 3′,3′-dipropyloxacarbocyanine; CAT, chloramphenicol acetyltransferase; Qac, quaternary ammonium compound.

10.1021/bi035447+ CCC: $25.00
Published on Web 12/03/2003

Table 1: Plasmids Used in This Study

plasmid	description	reference
pBluescript KS$^+$	*E. coli* cloning vector	Stratagene
pRB394	source of pUB110 *cat* gene	*32*
pSK1	*S. aureus* multiresistance plasmid conferring trimethoprim, gentamicin, and multidrug resistance	*45*
pSK412	pBR322 containing the 5.33 kb *Hin*dIII *qacA*−*qacR* encoding fragment from pSK1, source of *qacA*−*qacR* DNA	*33*
pSK5201	source of *rrnB*T1 transcription terminator	*16*
pSK5676	construct for overexpression of cysteine-less QacR	*17*
pSK5726	*Spe*I−*Kpn*I PCR clone of *qacR*−P$_{qacA}$ in pBluescript KS$^+$	this study
pSK5728	*Pst*I−*Kpn*I PCR clone of pUB110 *cat* gene in pUC19	this study
pSK5731	pSK5728 with *rrnB*T1 terminator inserted downstream of *cat*	this study
pSK5733	pSK5726 with *Pst*I−*Kpn*I *cat*−*rrnB*T1 fragment from pSK5731 fused to P$_{qacA}$	this study
pSK5743	pBluescript KS$^+$ derivative with *Eco*RI and *Kpn*I sites eliminated	this study
pSK5750	5.33 kb *qacA*−*qacR* *Hin*dIII fragment from pSK412 inserted into pSK5743	this study
pSK5751	pSK5750 with *Eco*RI−*Kpn*I fragment replaced with P$_{qacA}$−*cat*−*rrnB*T1 fragment from pSK5733	this study
pSK5754	pSK1 containing P$_{qacA}$−*cat* fusion introduced by homologous recombination with pSK5751	this study
pUC19	*E. coli* cloning vector	*46*

examples where a natural MDR pump substrate has also been documented to cause induction of expression via a well-characterized mechanism has been difficult to obtain. For example, despite spermidine representing the only natural substrate identified to date for the *B. subtilis* Blt MDR transporter (*14*), spermidine and related polyamines are not bound by the BltR local regulatory protein; in fact, these compounds fail to cause induction of *blt* expression by any mechanism (*15*). However, a more promising example is provided by the *S. aureus qacA*−*qacR* locus, for which the plant alkaloid berberine has been shown to be a substrate of the QacA MDR pump (*12*), in addition to the QacR regulatory protein possessing a demonstrated ability to bind berberine in vitro (*8*).

The QacR protein is a TetR family member that negatively regulates transcription of the divergently encoded QacA MDR pump by binding as a pair of dimers to the IR1 operator sequence, a large inverted repeat immediately upstream of the *qacA* promoter (P$_{qacA}$) (*16*, *17*). The structural basis for the conformational changes that occur within QacR upon binding QacA substrates, thereby resulting in QacR adopting a non-DNA-binding configuration and the concomitant derepression of P$_{qacA}$, has been recently elucidated (*18*). The *qacA*−*qacR* locus, which confers antiseptic and disinfectant resistance, is prevalent on multiresistance plasmids that are frequently isolated from clinical strains of *S. aureus* (*19*−*21*). The QacA integral membrane pump exports a wide range of toxic monovalent and bivalent lipophilic substrates, which includes more than 30 distinct compounds (*22*−*24*). Although fluorescent assays have been used to determine the kinetic parameters of transport, viz., the K_m and V_{max} values for QacA-mediated export of four fluorescent substrates, 4′,6-diamidino-2-phenylindole (DAPI), 3′,3′-dipropyloxacarbocyanine ($DiOC_3$), ethidium, and pyronin Y (*22*), relatively little is known about the range of compounds bound by the QacR regulatory protein and almost nothing regarding the relative affinity of QacR for various ligands. Furthermore, although a crystal structure exists for QacR bound to the plant alkaloid berberine (*8*), no data have been published on the ability of berberine to cause induction of *qacA* expression in vivo or on the in vitro binding affinity of QacR for this compound. In fact, the only published binding affinity determined to date has been that for rhodamine 6G, determined by equilibrium dialysis (*8*). In this paper, we address the lack of information available for QacR−ligand interactions by reporting on the abilities of an impressive range of structurally diverse compounds to induce expression of *qacA* transcription in the native Gram-positive *S. aureus* host, since the induction of *qacA* expression has only previously been investigated with a limited range of compounds (*16*, *25*). These results are confirmed in vitro by demonstrating the dissociation of QacR from IR1 operator DNA in the presence of inducers. A ligand-binding assay based on intrinsic tryptophan fluorescence was also developed to determine the relative affinities of the QacR protein for these same ligands, which included a number of natural plant alkaloids.

EXPERIMENTAL PROCEDURES

Bacterial Strains and Growth Conditions. All cloning and overexpression procedures performed in *Escherichia coli* utilized strain DH5α (*26*), whereas two *S. aureus* strains were employed, RN4220 (*27*) and the *norA* multidrug efflux pump determinant knockout SAK1712 (*28*). Unless stated otherwise, all strains were cultured at 37 °C in Luria−Bertani broth or agar (*26*) containing, where appropriate, 100 μg mL^{-1} ampicillin for *E. coli* and 50 μg mL^{-1} ethidium, 25 μg mL^{-1} gentamicin, 3 μg mL^{-1} tetracycline, or 100 μg mL^{-1} trimethoprim for *S. aureus*. *E. coli* was transformed by standard procedures (*26*) and *S. aureus* by electroporation as previously described (*29*), employing a pulse of 1.3 kV. Plasmids used in this study are listed in Table 1.

DNA Manipulations. Plasmid DNA was isolated from *E. coli* and *S. aureus* using the Quantum Prep kit (Bio-Rad) and small-scale alkaline lysis (*30*), respectively. Restriction enzymes, T4 DNA ligase, the Klenow fragment of DNA polymerase I (all from New England Biolabs), shrimp alkaline phosphatase (Promega), *Pfu* DNA polymerase (Stratagene), and the Wizard PCR purification kit (Promega) were each used according to the manufacturers' instructions. Oligonucleotides were purchased from Sigma, and automated DNA sequencing was performed at the Australian Genome Research Facility.

Production of a P$_{qacA}$−cat Reporter Gene Fusion. A 0.8 kb PCR fragment encompassing a promoter-less pUB110 *cat* gene (*31*), but retaining its ribosome-binding site, was amplified from pRB394 (*32*) template DNA by PCR, employing the oligonucleotide pair 5′-GACCTGCAGAAGCTTAGCTAGTTAAAATTTAGGAGGAATTTATATATGAC-

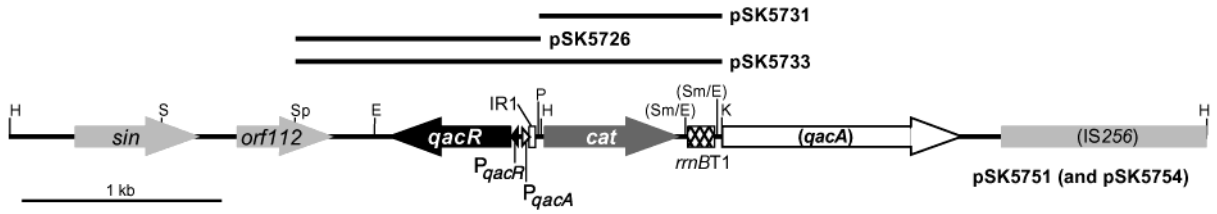

FIGURE 1: Linear map of pSK5751 insert DNA, which was subsequently recombined into pSK1 to generate the P_{qacA}−*cat* fusion derivative pSK5754. Shown is the *qacR* gene (black arrow), its promoter P_{qacR}, the *qacA* operator DNA-binding site IR1, the fusion of the *qacA* promoter (P_{qacA}) to a *cat* reporter gene (dark gray arrow), the downstream *rrnB*T1 transcription terminator (crosshatched box), the truncated *qacA* gene (white arrow), and the *sin* and *orf112* genes (light gray arrows), which together with the majority of an IS*256* insertion sequence (light gray rectangle) are encoded by the DNA flanking the site of the reporter gene fusion. The portions of pSK5751 which are contained by the constructs pSK5726, pSK5731, and pSK5733 are also delineated, with a bar indicating 1 kb. Restriction endonuclease sites: E, *Eco*RI; H, *Hin*dIII; K, *Kpn*I; P, *Pst*I; S, *Sal*I; Sm, *Sma*I; Sp, *Spe*I (those in parentheses were removed during the cloning process).

3′ and 5′-TTAGGTACCCGGGCAGTTTATGGCGGGCGTCCTGC-3′ (underlined nucleotides represent inserted restriction endonuclease recognition sites) and then cloned into the *Pst*I and *Kpn*I sites of pUC19 to produce pSK5728. A 0.16 kb *Eco*RI fragment encompassing a *rrnBT1* transcription terminator was acquired from pSK5201 (*16*), blunt-ended, and inserted downstream from the *cat* gene in pSK5728 by way of the *Sma*I site previously introduced by the 3′ PCR primer, thereby generating pSK5731 (Figure 1). To obtain a P_{qacA}-containing fragment suitable for fusing to the promoterless *cat* gene, the 5.33 kb *Hin*dIII *qacA*−*qacR* containing DNA segment from pSK412 (*33*) was first recloned into the *Hin*dIII site of pSK5743 (Table 1). The resultant plasmid, pSK5750, was subsequently used as the template DNA for a PCR reaction with the oligonucleotide pair 5′-CCGGAAGCTTGGGTACCAATCCTTATAGACCGTG-3′ and 5′-GAAAAAGGCGTATATATAAAGG-3′, resulting in the generation of a 1.84 kb fragment. After cleavage of the PCR product with *Spe*I and *Kpn*I, the released 1.21 kb *qacR*−P_{qacA} fragment was cloned into the equivalent sites of pBluescript KS^+ to produce pSK5726 (Figure 1). The unique *Pst*I and *Kpn*I sites, incorporated by the 3′ PCR primer, were then utilized to insert the *cat*−*rrnB*T1 fragment from pSK5731, thereby generating pSK5733 (Figure 1), which contained a fusion of the *cat* reporter gene to P_{qacA}. The final product, pSK5751 (Figure 1), was created by replacement of the pSK5750 *Eco*RI−*Kpn*I fragment with that from pSK5733. After the electroporation of pSK5751 DNA into *S. aureus* strain RN4220 harboring pSK1, the pSK1 derivative pSK5754 was isolated, in which the P_{qacA}−*cat* fusion had replaced the wild-type sequences by homologous recombination.

Chloramphenicol Acetyltransferase Assays. A stationary-phase culture of *S. aureus* strain SAK1712 harboring pSK5754 was diluted 1:100 in fresh media and grown to an OD_{600} of 0.6, which equated to approximately five population doublings and mid-log phase of growth (data not shown). Aliquots (3 mL) were then grown for a further 1.5 h in the presence or absence of the indicated concentrations of potential inducing compounds and placed on ice. Cells lysis was achieved by resuspension in 300 μL of cold buffer (10 mM EDTA, 25 mM Tris-HCl, pH 8.0) containing 0.3 mg mL^{-1} lysostaphin and incubation at 37 °C for 30 min. After centrifugation, 50 μL samples of supernatant were added to spectrophotometer tubes containing 2900 μL of chloramphenicol acetyltransfersase (CAT) assay buffer, such that the final concentrations were 100 mM Tris-HCl, pH 7.8, 0.1 mM acetyl-CoA (Sigma), and 1 mM 5,5′-dithiobis(2-nitrobenzoic acid) (Sigma). Reactions were equilibrated for 5 min at 37 °C, and a zero reading was obtained by measuring absorbance at 412 nm in a Spectronic 20 spectrophotometer at 37 °C before the addition of 0.15 mM chloramphenicol (Sigma) followed by a second reading after a further 5 min incubation at 37 °C. The concentration of protein in each sample supernatant was determined with the Coomassie plus protein assay reagent (Pierce), permitting the obtained CAT activities to be expressed as μM Cm acetylated min^{-1} (mg of protein)$^{-1}$. Potential inducing compounds were obtained from the following sources: ampicillin, benzalkonium chloride, berberine chloride, cetylpyridinium chloride, chelerythrine chloride, chlorhexidine diacetate, crystal violet, DAPI, dequalinium chloride, $DiOC_3$, ethidium bromide, malachite green, methyl green, palmatine chloride, proflavin, pyronin Y, rhodamine 6G, tetracycline, and tetraphenylarsonium were all from Sigma Aldrich, amicarbalide isethionate, phenamidine isethionate, and propamidine isethionate were provided by Rhone Poulenc Rorer (Dagenham, U.K.), and the compounds avicin and nitidine were supplied by Drs. Monroe E. Wall and Mansukh C. Wani (Research Triangle Institute, Research Triangle Park, NC).

Protein Purification and Gel Mobility Shift Assays. The cysteine-less His tag derivative of QacR used throughout this work was overexpressed from the plasmid pSK5676 and purified by Ni^{2+}-NTA metal chelate affinity chromatography (Invitrogen ProBond resin) as described previously (*16*, *17*). Immediately following elution from the column, the QacR-containing fractions were pooled, diluted to a concentration not exceeding 1 mg mL^{-1}, and dialyzed for at least 4 h at room temperature against 4 L of buffer A [200 mM NaCl, 20 mM Tris-HCl, 5% (v/v) glycerol, pH 7.5] to remove imidazole. After a second, overnight dialysis against fresh buffer A, the QacR-containing solution was 0.22 μm filtered (Millipore GS) and stored in single use aliquots at −70 °C. Protein concentrations were determined using the Coomassie plus protein assay reagent (Pierce), and in selected instances their accuracy was verified by measurement of absorbance at 205 nm in a solution of 0.01% Brij 35 (Sigma) (*34*). Gel mobility shift assays, for the purposes of assessing the activity of purified QacR preparations, and also to determine the ability of newly identified QacR ligands to dissociate QacR dimers from operator DNA, were performed, utilizing a 137-bp γ-^{32}P-labeled P_{qacA}−IR1 operator DNA fragment as described previously (*16*).

Fluorescence Spectroscopy. Fluorescence intensity measurements were made at room temperature with a Hitachi F-4500 fluorescence spectrophotometer employing a 1 cm × 1 cm quartz cell. Tryptophan residues in QacR were selectively excited at 295 nm, and the emission was monitored at 340 nm with slit widths of 5 and 10 nm, respectively. Stocks of ligands (2.5 mM) were dissolved in DMSO and dilutions made as required in buffer B [100 mM NaCl, 15 mM Tris-HCl, 2.5% (v/v) glycerol, pH 7.5]. Dialyzed QacR was added to buffer B at a concentration of approximately 15 μg mL^{-1} (0.32 μM dimer = [QacR]) in an initial volume of 2 mL and titrated with increasing amounts of each ligand by the sequential addition of 2−4 μL aliquots of the appropriate ligand stock solutions, such that the total addition of ligand did not exceed 5% of the initial volume. All readings were corrected for background emission of the buffer and sample dilution. Inner filter effects were compensated for by performing a parallel titration using a 1 μM solution of pure tryptophan (Sigma), which produced an initial fluorescence intensity reading approximately equivalent to that obtained for the 15 μg mL^{-1} QacR samples. The reductions in the tryptophan fluorescence intensity were assumed to be entirely due to inner filter effects, and these data were then used to obtain corrected fluorescence quenching values (ΔF_C) for the titrations of QacR with ligand by employing the equation:

$$\Delta F_C = \frac{\Delta F_P - F_{Pi}(\Delta F_W/F_{Wi})}{F_{Pi}} \quad (1)$$

where ΔF_P = the reduction in QacR fluorescence intensity at a particular concentration of ligand, F_{Pi} = the initial fluorescence of QacR, ΔF_W = the reduction in tryptophan fluorescence intensity at a particular concentration of ligand, and F_{Wi} = the initial fluorescence of the tryptophan solution.

K_d Determinations. The fraction of QacR dimers containing a bound ligand molecule (ΔF^*) was taken as the fraction of the total quenchable tryptophan fluorescence that was quenched at each point of the titration. To calculate ΔF^* values, the total quenchable signal was first estimated by extrapolation at high [L] values to the *Y*-intercept of a plot of 1/[L] vs 1/ΔF_C. For each point in a titration, the concentration of free ligand [L_f] was also approximated by subtracting from the total ligand concentration (in μM), [L], the concentration of ligand molecules estimated to be bound by QacR, ([QacR]ΔF^*), based on the previously determined binding stoichiometry of one ligand molecule per QacR dimer (*8*). Dissociation constants for each ligand were then determined by using the nonlinear curve least-squares fitting program EnzFitter (Biosoft, Cambridge, U.K.) to fit the experimental [L_f] and ΔF^* values to a single-site ligand-binding model (eq 2), with each of the reported K_d values representing an average from three separate K_d determinations:

$$\Delta F^* = \Delta F^*_{max}\frac{[L_f]}{[L_f] - K_d} \quad (2)$$

RESULTS

Recombination of a P_{qacA}−cat Fusion into the pSK1 Multiresistance Plasmid. To obtain an accurate representation of *qacA* induction in *S. aureus*, a transcriptional fusion of a Gram-positive *cat* reporter gene to P_{qacA} was generated and the resultant construct recombined into the pSK1 multiresistance plasmid, the original source of the *qacA*−*qacR* locus. Briefly, a promoter-less pUB112 *cat* gene was first cloned in *E. coli* (pSK5728; Table 1) and then modified to include a downstream *rrnB*T1 transcription terminator (pSK5731; Table 1) in order to prevent the possible production of a truncated QacA protein, as it has been reported that the expression of truncated versions of other integral membrane proteins can be deleterious to the health of bacterial cells (*35*). After the fusion of the *cat* gene to a P_{qacA}−IR1 sequence with *qacR* in cis (pSK5733; Table 1), the quantity of pSK1 DNA flanking the *cat* gene was increased so as to facilitate the planned homologous recombination event. These manipulations culminated in the production of pSK5751, in which the P_{qacA}−*cat* fusion was flanked by 2.64 and 2.52 kb of pSK1 DNA upstream and downstream of *cat*, respectively (Figure 1). After electroporation of pSK5751 DNA into an *S. aureus* RN4220 derivative that already harbored pSK1, recombinant plasmids were selected by plating the cells on NYE agar (*29*) containing 25 μg mL^{-1} gentamicin and 100 μg mL^{-1} trimethoprim to select for pSK1, in addition to 5 μg mL^{-1} chloramphenicol and a subminimum inhibitory concentration (10 μg mL^{-1}) of proflavin, a compound previously shown to cause induction of transcription from P_{qacA} (*16*). Because pSK5751 lacked *S. aureus* replication functions, the obtained chloramphenicol-resistant colonies should be the product of the desired recombination event. Indeed, this appeared to be the case, as each isolate possessed a plasmid marginally larger in size than pSK1, as would be expected for the additional 0.82 kb of DNA that resulted from the insertion of the *cat* gene and concomitant deletion of the first 157 bp of the *qacA* gene. One of these pSK1 derivatives containing a P_{qacA}−*cat* fusion was designated pSK5754. Verification of a successful recombination event that disrupted the *qacA* gene was provided by the growth of RN4220 harboring pSK1, but not the equivalent strain containing pSK5754, in the presence of 100 μg mL^{-1} ethidium or 100 μg mL^{-1} proflavin, compounds which are substrates of the QacA MDR pump (*22*). The integrity of the DNA surrounding the fusion site was validated by PCR, with the appropriately sized fragment being obtained in each case, in addition to the verification of the DNA sequence for the segment that encompassed *qacR*, the intergenic region, and the *cat* gene (data not shown).

Induction of qacA Expression in S. aureus. The *S. aureus* chromosomally encoded NorA MDR pump shares a number of common substrates with the QacA MDR transporter, such as tetraphenylarsonium, benzalkonium, rhodamine 6G, and ethidium (*22*, *36*, *37*). To avoid expression of NorA from potentially masking the ability of some compounds to act as inducers of *qacA* transcription, the *S. aureus* strain SAK1712 (*28*) was employed, in which the *norA* coding region has been disrupted by the insertion of the pT181-derived TetA(K) tetracycline resistance cassette. The high specificity of the pT181-encoded efflux protein for only tetracycline and some closely related analogues (*38*) precluded any influence on the intracellular concentrations of the compounds analyzed in this study. After transformation of strain SAK1712 with pSK5754, a resultant transformant

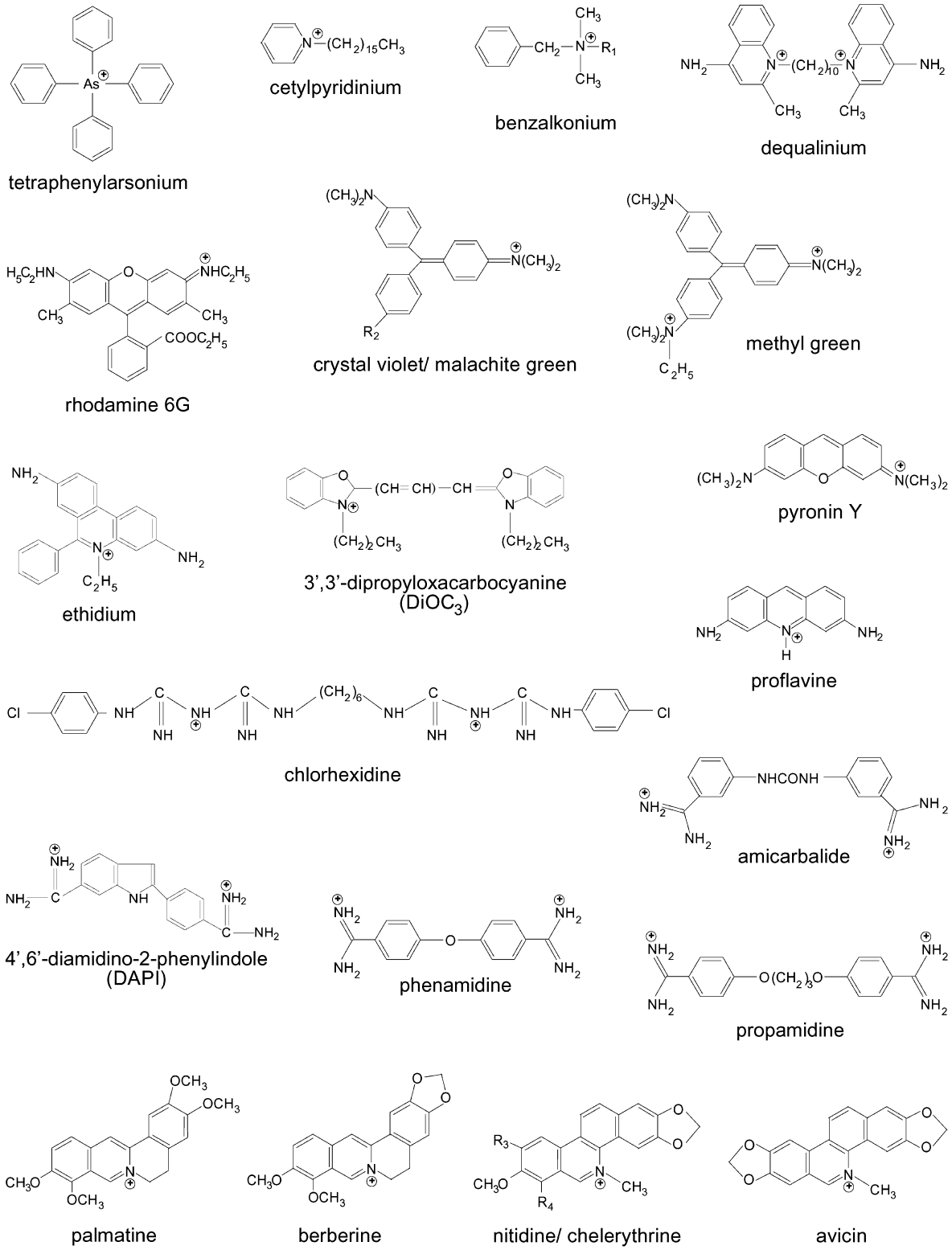

FIGURE 2: Chemical structures of QacR ligands. Depicted are the monovalent Qacs tetraphenylarsonium, cetylpyridinium, and benzalkonium (R_1 = $C_{12}H_{25}$, $C_{14}H_{29}$, or $C_{16}H_{33}$), the bivalent Qac dequalinium, the monovalent dyes rhodamine 6G, crystal violet [R_2 = $N(CH_3)_2$], malachite green (R_2 = H), ethidium, $DiOC_3$, pyronin Y, and proflavin, the bivalent dye methyl green, the bivalent guanidine chlorhexidine, the bivalent diamidines amicarbalide, DAPI, phenamidine, and propamidine, and the plant alkaloids palmatine, berberine, nitidine (R_3 = OCH_3, R_4 = H), chelerythrine (R_3 = H, R_4 = OCH_3), and avicin.

was employed for CAT assays to determine the ability of structurally diverse compounds to act as inducers of *qacA* transcription. The potential QacR ligands assessed included a number of recently identified monovalent and bivalent QacA substrates (*23*) and a range of natural plant alkaloids which share some structural similarities with known synthetic QacR ligands (Figure 2).

Initially, as a control, the *S. aureus* strain SAK1712 harboring pSK1 was used in CAT assays; no CAT activity was detectable, a result which did not change upon the

addition of known QacR ligands (data not shown). In comparison, even in the absence of inducing compounds, a significant basal level of CAT activity was detected for SAK1712 harboring pSK5754 (Figure 3). More importantly, upon addition of many of the potential QacR ligands, substantial increases in transcription from P_{qacA} were observed (Figure 3), the maximal levels of which were classified either as a low (less than 2-fold), moderate (2−3-fold), or strong (greater than 3-fold) increase in the basal expression (Table 2). For example, addition of increasing amounts of the strong inducer methyl green, a bivalent dye, resulted in a gradual increase in the detected CAT activity, from a basal level of 125 units to a maximum of 398 units at 31 μM methyl green (Figure 3B and Table 2). Other compounds classified as strong inducers were the monovalent dyes rhodamine 6G and $DiOC_3$ (Figure 3B), the monovalent quaternary ammonium compound (Qac) tetraphenylarsonium, the bivalent Qac dequalinium (Figure 3D), and the plant alkaloid berberine (Figure 3C). The monovalent Qac benzalkonium (Figure 3D), the monovalent dye crystal violet (Figure 3B), and the plant alkaloids nitidine and palmatine (Figure 3C) were all moderate inducers of P_{qacA} expression. Weak inducers of P_{qacA} expression included the monovalent dyes proflavin, pyronin Y, and ethidium (Figure 3A), the bivalent guanidine chlorhexidine (Figure 3E), and the bivalent diamidine DAPI (Figure 3E). The sharp drop-off in CAT activity seen with many compounds at higher concentrations is explained by the inhibitory effect on cell growth that was observed at these high levels of inducer (data not shown). The inducing status of the monovalent dye malachite green (Figure 3B and Table 2), the plant alkaloids chelerythrine (Figure 3C) and avicin (Table 2), the Qac cetylpyridinium (Figure 3D), and the diamidines amicarbalide, propamidine, and phenamidine (Figure 3E and Table 2) was unclear, as after an initial drop in CAT activity, they each only caused a small increase in transcription from P_{qacA}, such that it did not substantially exceed the value obtained in the absence of any inducing compound. The addition of ampicillin and tetracycline, representing control antimicrobials which are not QacA substrates, failed to cause an increase in *qacA* expression (data not shown).

Gel Mobility Shift. To confirm that the observed increases in *qacA* expression represented a direct interaction with QacR, the ability of compounds to dissociate purified QacR protein from IR1-containing DNA was assessed by gel mobility shift analysis for all of the newly identified inducers. All compounds which had a significant effect on P_{qacA} transcription in vivo were found to also inhibit binding of QacR to P_{qacA}−IR1 containing probe DNA in vitro (Figure 4). Interestingly, one of the weakest inducers, pyronin Y, had a significant in vitro effect at less than 100 μM (Figure 4A), requiring a lower concentration than the strongest inducer, $DiOC_3$ (Figure 3B), to completely dissociate QacR from IR1. Similarly, although the maximal induction by methyl green occurred at a concentration 6-fold greater than that required for $DiOC_3$ (Table 2), the former compound completely dissociated QacR from operator DNA at a much lower concentration than the latter (Figure 4A). Because excess concentrations of the control noninducing antimicrobials ampicillin, tetracycline, and chloramphenicol did not dissociate QacR from IR1 DNA (Figure 4B), it indicated that the effects observed upon addition of the plant alkaloids chelerythrine and avicin, as well as the diamidines amicarbalide, phenamidine, and propamidine (Figure 4), represented a real interaction with QacR, despite these compounds only inducing poorly or not at all in vivo (Figure 3).

Ligand-Binding Assay: Intrinsic Tryptophan Fluorescence. QacR contains three highly fluorescent tryptophan residues, one of which is known to directly participate in ligand binding (*8*). Therefore, it appeared probable that an assay based on the intrinsic fluorescence of QacR could be developed to measure the relative binding affinities of QacR for different ligands. Although QacR possesses two ligand-binding pockets per dimer, the structural information available for six different ligands indicated that, in each case, binding of the ligand to one site caused nearly identical structural changes, which sterically hindered access of ligands to the second site (*8*). For the compound rhodamine 6G, a binding stoichiometry of one molecule per QacR dimer had been confirmed by equilibrium dialysis (*8*). Thus, the fluorescence quenching data obtained from titration of QacR with ligands were fitted to a single-site ligand-binding model.

Initial experiments revealed that the tryptophan fluorescence of QacR could be readily quenched by the addition of submicromolar to low micromolar concentrations of rhodamine 6G in a concentration-dependent manner (Figure 5A), whereas the same concentrations of rhodamine 6G had little effect on the fluorescence of a solution of pure tryptophan (Figure 5A). Fitting of the corrected $[L_f]$ and ΔF^* values to a single-site binding model produced an excellent fit (Figure 5B), generating a dissociation constant (K_d) of 197 ± 15 nM, which is in good agreement with the value of 101 ± 4 nM previously determined for rhodamine 6G by equilibrium dialysis (*8*).

The binding assay was successfully employed to determine K_d values for the majority of compounds known to cause induction of *qacA* expression in vivo (Figure 3) and/or dissociation of QacR from IR1 operator DNA in vitro (Figure 4) (*16*). Unfortunately, dequalinium and propamidine both exhibited significant fluorescence at 340 nm, and addition of benzalkonium caused a slight increase of QacR fluorescence; QacR binding of these compounds could not be studied with this method. The results of K_d determinations for the 14 monovalent and 5 bivalent compounds are presented in Table 2. The two compounds which were clearly bound the strongest by QacR, crystal violet and rhodamine 6G, are both monovalent dyes, although their chemical structures are rather disparate (Figure 2). The other five monovalent dyes and the Qac cetylpyridinium were also bound relatively strongly by QacR (Table 2), whereas the bivalent dye methyl green had a significantly higher K_d of 7.04 ± 2.69 μM. In fact, with the exception of DAPI, all of the bivalent compounds had relatively high K_d values, irrespective of the class of the compound; tetraphenylarsonium was the only monovalent compound found to be bound more weakly (Table 2). The five plant alkaloids tested exhibited similar K_d values to each other, from a low of 2.63 ± 0.13 μM for avicin to a high of 4.89 ± 0.83 μM for nitidine (Table 2). However, it should be noted that only approximate values could be obtained for the plant alkaloids berberine and palmatine, due to the severity of the inner filter effects for these compounds, such that a marked reduction in the fluorescence of free tryptophan was observed.

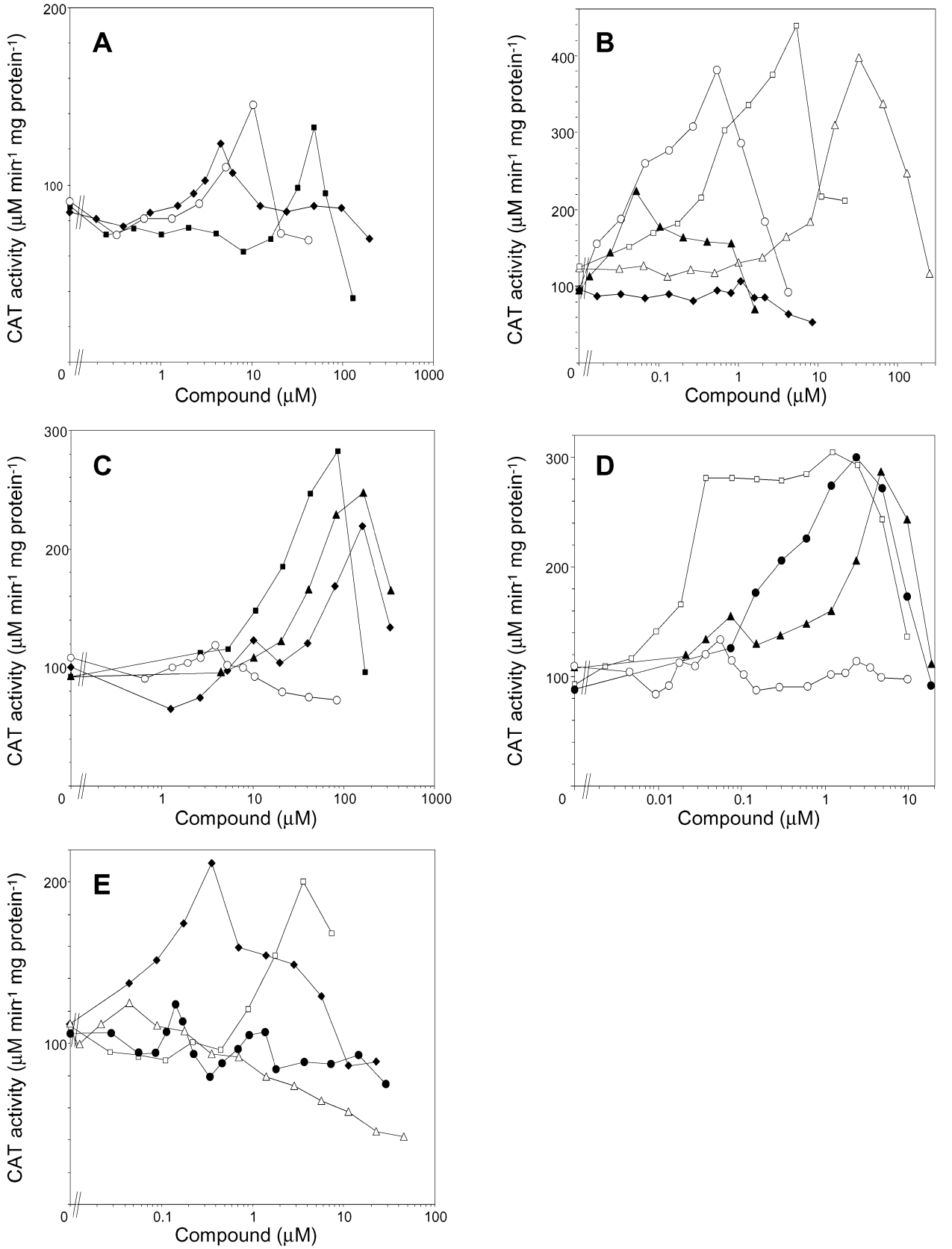

FIGURE 3: Induction of transcription from the P_{qacA}−*cat* fusion in pSK5754 following the addition of potential QacR ligands, determined in the *S. aureus norA* knockout strain SAK1712. (A) Monovalent dyes proflavin (filled diamonds), pyronin Y (open circles), and ethidium (filled squares). (B) Monovalent dyes crystal violet (filled triangles), malachite green (filled diamonds), rhodamine 6G (open circles), and $DiOC_3$ (open squares) and the bivalent dye methyl green (open triangles). (C) Monovalent plant alkaloids berberine (filled squares), palmatine (filled triangles), nitidine (filled diamonds), and chelerythrine (open circles). (D) Bivalent Qac dequalinium (open squares) and the monovalent Qacs tetraphenylarsonium (filled circles), benzalkonium (filled triangles), and cetylpyridinium (open circles). (E) Bivalent guanidine chlorhexidine (open squares) and the bivalent diamidines DAPI (filled diamonds), amicarbalide (filled circles), and propamidine (open triangles).

Table 2: Ligand-Binding Affinities of QacR and Maximum Fold in Vivo Induction

compound	binding affinity (μM) (K_d)[a]	maximum in vivo induction[b]	
		x-fold increase	concn (μM)
dyes			
crystal violet	0.3 ± 0.02	2.4	0.05
$DiOC_3$[c]	1.77 ± 0.22	3.5	5.2
ethidium	0.81 ± 0.24	1.5	49
malachite green	1.76 ± 1.05	1.1	1.0
methyl green[c]	7.04 ± 2.69	3.2	31
proflavin	3.15 ± 0.639	1.4	4.6
pyronin Y	5.15 ± 0.47	1.6	10
rhodamine 6G	0.20 ± 0.02	4.1	0.52
quaternary ammonium compounds			
benzalkonium	nd[d]	2.6	4.7
cetylpyridinium	0.47 ± 0.05	1.2	0.05
dequalinium[c]	nd[d]	3.3	1.2
tetraphenylarsonium	81.78 ± 11.27	3.4	2.4
guanidines			
chlorhexidine[c]	11.42 ± 0.63	1.8	3.2
diamidines			
amicarbalide[c]	16.21 ± 0.53	1.2	0.14
DAPI[c]	1.12 ± 0.18	1.9	0.36
phenamidine[c]	9.21 ± 0.35	0.93	1.9
propamidine[c]	nd[d]	0.83	0.35
plant alkaloids			
avicin	2.63 ± 0.13	1.1	10
berberine[e]	2.88 ± 0.52	3.1	86
chelerythrine	4.08 ± 1.07	1.1	3.9
nitidine	4.89 ± 0.83	2.2	160
palmatine[e]	3.74 ± 0.67	2.7	170

[a] Values are an average from three separate experiments. [b] Values represent the maximum level of CAT activity observed in the presence of each compound such that a value of 1 represents the level of transcription originating from P_{qacA} in the absence of any inducing compound. Also recorded is the corresponding optimum concentration for each compound (Figure 3 and data not shown). [c] Bivalent compounds. [d] Not determined (see text). [e] Due to the severity of the inner filter effect, only approximate K_d values could be determined for berberine and palmatine.

DISCUSSION

This paper proffers the first detailed study of the range of compounds bound by the multiligand-binding repressor QacR. Application of the P_{qacA}−*cat* reporter gene fusion provided an accurate picture of induction from the *qacA* promoter when both P_{qacA} and the divergently transcribed *qacR* gene were present in their natural location in the pSK1 multiresistance plasmid (Figure 3) and expressed in the native staphylococcal host. Variance from data previously obtained using an *E. coli* promoter-probe vector (*16*) may well be attributable to the outer membrane of Gram-negative organisms, which provides *E. coli* with an added barrier to the entry of antimicrobial compounds. Additionally, the employment of an *S. aureus norA* knockout mutant may also have increased the sensitivity of the *qacA* induction assays. For example, the bivalent biguanidine chlorhexidine, which had previously been classified as noninducing and represents a chemical class distinct from that of other inducers (Figure 2), has now been unambiguously reclassified as an inducing compound. Chlorhexidine was observed to cause a low but significant increase in the level of P_{qacA} transcription (Table 2; 1.8-fold), a result which was supported by the ability of chlorhexidine to dissociate QacR from IR1 DNA in vitro

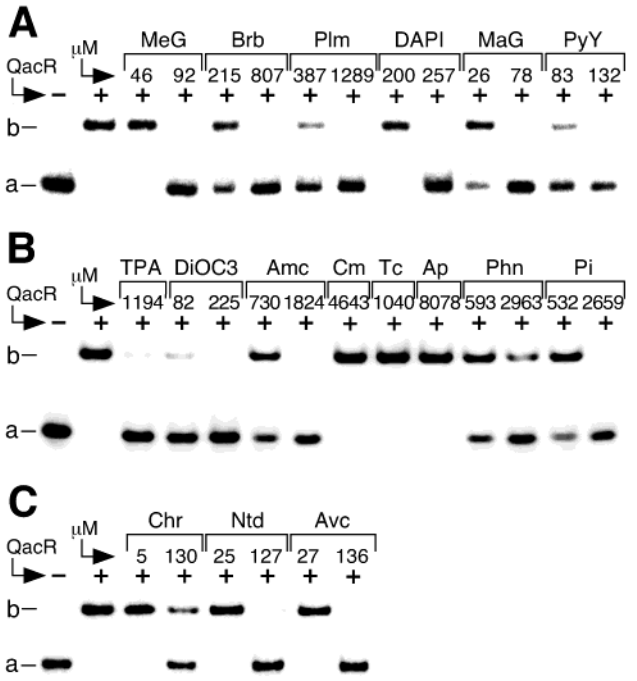

FIGURE 4: Gel mobility shift assays demonstrating dissociation of QacR from IR1 operator DNA in vitro following the addition of QacR ligands. 500 cpm of a ^{32}P-labeled 137-bp P_{qacA}-IR1 containing fragment (a) was incubated in the presence (+) or absence (−) of 0.4 ng of purified QacR and in some cases with the addition of the indicated concentrations (in μM) of potential QacR ligands. Formation of a QacR−IR1 DNA complex (b) retarded the degree to which the probe DNA migrated into the gel. QacR ligands are abbreviated as follows: Amc, amicarbalide; Ap, ampicillin; Avc, avicin; Brb, berberine; Chr, chlorhexidine; Cm, chloramphenicol; MaG, malachite green; MeG, methyl green; Ntd, nitidine; Phn, phenamidine; Pi, propamidine; Plm, palmatine; PyY, pyronin Y; Tc, tetracycline; TPA, tetraphenylarsonium

(*16*) and the determination of a K_d value of 11.42 ± 0.63 μM (Table 2). In a similar fashion, what appeared to be a low level of induction by the Qac cetylpyridinium (Table 2; 1.2-fold) was also matched by the ability of this compound to both bind QacR in vitro (Table 2; K_d of 0.47 ± 0.05 μM) and dissociate it from IR1 DNA (*16*). Compounds that were capable of mediating 1.6- and 3.5-fold increases in *qacA* transcription, respectively, also included the newly identified inducers pyronin Y and $DiOC_3$, both of which are monovalent dyes that had K_d values in the low micromolar range (Table 2).

The bivalent dye methyl green is highly similar in structure to the monovalent compounds crystal violet and malachite green (Figure 2) and represents the first example of a QacR ligand that is not itself a substrate of the QacA transporter (B. A. Mitchell, M. H. Brown, and R. A. Skurray, unpublished data). Induction by methyl green required relatively high concentrations (Figure 3B and Table 2), in line with the higher K_d value obtained for this compound (Table 2; 7.04 ± 2.69 μM). However, in comparison to these methyl green results, the K_d values in general did not correlate very well with the strength of in vivo induction. For example, the newly identified inducer tetraphenylarsonium had the highest K_d (Table 2; 81.78 ± 11.27 μM) and required a substantial concentration to disrupt QacR−IR1 complexes (Figure 4B) but exhibited strong in vivo induction (Table 2; 3.4-fold). In contrast, cetylpyridinium only induced very

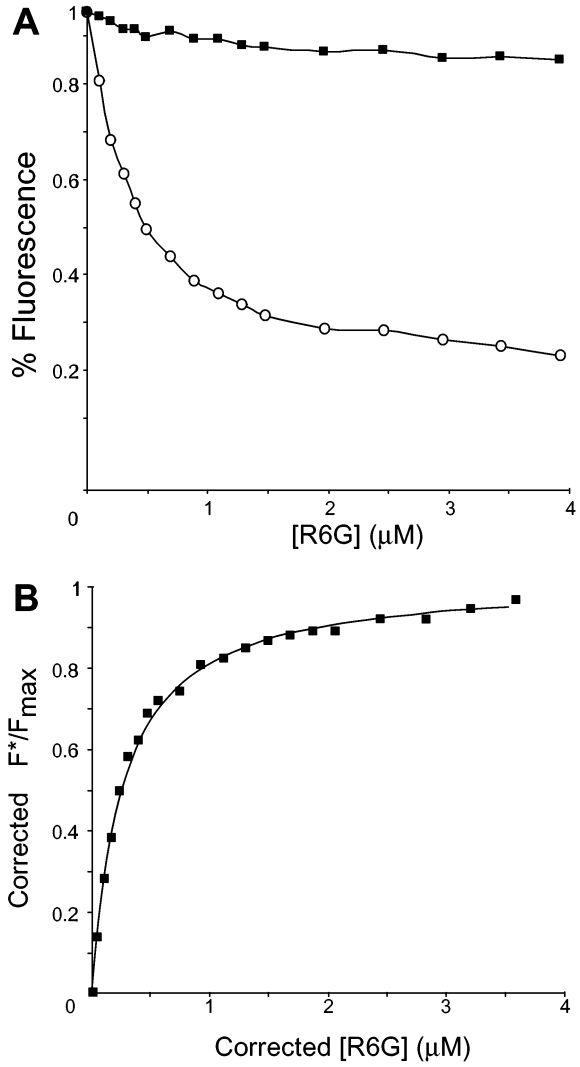

FIGURE 5: Binding of the ligand rhodamine 6G to QacR determined by quenching of intrinsic tryptophan fluorescence. (A) Fluorescence quenching of QacR (diamonds) and free tryptophan (squares) by the addition of increasing amounts of rhodamine 6G, with λ_{ex} set at 295 nm and λ_{em} at 340 nm. (B) Determination of the dissociation constant (K_d) for rhodamine 6G. At each point in the titration shown in (A), the QacR fluorescence values were corrected for inner filter effects using eq 1 in the Experimental Procedures, and the free rhodamine 6G concentration was adjusted for the estimated quantity of ligand bound by QacR. The proportion of the quenchable QacR fluorescence signal (ΔF^*) quenched at each step in the titration and the corresponding values for the free ligand concentrations [$R6G_{free}$] were then fitted to eq 2 of the Experimental Procedures. The points represent the data derived from (A), with the line representing the best fit of these data to eq 2, in this instance generating a K_d value for rhodamine 6G of 198 nM.

poorly (Figure 3D and Table 2; 1.2-fold), despite a demonstration of strong in vitro binding (Table 2; K_d of 0.47 ± 0.05 μM) (*16*). A range of bivalent diamidines, including the structurally distinct compound DAPI, were also identified as ligands of QacR (Figures 3E and 4A). DAPI bound significantly more tightly to QacR than the other bivalent compounds (Table 2; K_d of 1.12 ± 0.18 μM), suggesting a more precise fit of this compound in the extended QacR ligand-binding pocket. The limited level of induction observed for the other diamidines, viz., amicarbalide, phenamidine, and propamidine, ranging from 0.83-fold to 1.2-fold (Table 2), may reflect the concentrations that were required to observe an in vitro effect on DNA binding (Figure 4) vastly exceeding the maximum concentration at which they could be employed in vivo (Figure 3). In addition to toxicity, there are several other explanations which can account for a failure to observe significant in vivo induction for a compound that can readily dissociate QacR from IR1 DNA in vitro. For example, the ability of a given ligand to enhance *qacA* transcription is related not only to how strongly it is bound by QacR but also to the relative affinity of the compound for its target site, the ease with which it gains entry into the cytoplasm, and the presence of MDR transporter homologues which may export the compound in question, thereby reducing its intracellular concentration. For the specific case of ethidium, proflavin, and pyronin Y, the discrepancy between their relatively low K_d values, ranging from 0.81 to 5.15 μM, but only weak induction of P_{qacA} in vivo (Table 2) may be related to the ability of these compounds to intercalate DNA (*39*). This property could result in a reduction in the effective intracellular concentrations of such QacR ligands due to their nonspecific sequestration in chromosomal DNA. Although DNA intercalation could also enhance the effect of these compounds in gel mobility shift experiments, it does not influence the finding that QacR has a strong affinity for these ligands, as determined by the intrinsic tryptophan fluorescence assay (Table 2).

Taking into account the data presented here, the number of bivalent compounds that QacR is known to be capable of binding has now increased from a sole example, dequalinium, to seven, which in combination with the additional monovalent ligands that were identified indicates that the range of compounds bound by QacR is substantially greater than previously thought. This finding is particularly interesting in light of the fact that QacR also regulates the expression of QacB, a closely related protein from which QacA appears to have recently evolved via the acquisition of a high-affinity binding site for bivalent substrates (*20*, *22*, *40*). Importantly, although all of the known bivalent ligands of QacR, with the exception of methyl green, are also substrates of QacA, these same bivalent compounds are very poor substrates of QacB. Thus, it appears likely that the QacR regulator possessed bivalent cation-binding ability prior to the acquisition by QacA of a high-affinity bivalent substrate-binding site. Furthermore, an inability to induce *qacA* transcription does not mean that a compound should be disregarded as an important QacA substrate, as a significant degree of QacA-mediated resistance to a noninducing compound, such as phenamidine (*23*), can still occur in the absence of induction. This situation arises from the finding that although the *qacA* promoter drives relatively strong transcription in *S. aureus* (*41*), full repression by QacR only results in a 6-fold decrease in promoter activity (*41*). The significant basal level of transcription from uninduced P_{qacA} was also clearly demonstrated by the P_{qacA}−*cat* fusion generated in this study (Figure 3).

This study also clearly demonstrated for the first time in vivo induction of a bacterial MDR determinant by the natural plant antimicrobials berberine, palmatine, and nitidine (Figure 3C). QacR was confirmed to bind these plant alkaloids and the additional compounds, chelerythrine and avicin, in vitro (Figure 4), with K_d values in the low micromolar range (Table 2). In comparison, all other QacR ligands which have

been identified to date are artificial substances that have only recently been synthesized. This situation is at odds with the widespread distribution of MDR transporters (*42*), which suggests that these transporters are likely to have important physiological functions related to the export of unidentified substrates encountered in the normal environment of each organism. Although the ability of QacA to efflux palmatine, nitidine, avicin, and chelerythrine has yet to be investigated, at the very least, berberine is likely to represent a natural MDR substrate, as this plant alkaloid is a substrate of both the plasmid-encoded QacA and also the chromosomally encoded NorA *S. aureus* MDR pumps (*10*−*12*). Taken together, these findings are suggestive of a preexisting role for the QacA−QacR system in providing resistance to plant and other naturally occurring, cationic and hydrophobic, antimicrobial compounds. Thus, to provide resistance against antiseptics and disinfectants prevalent in the hospital environment, *S. aureus* appears to employ a system that may have evolved for the export of natural compounds which share broad chemical and structural similarities with many synthetic MDR transporter substrates (Figure 2). The high-affinity binding of both the QacA transporter and also the QacR regulator to the same range of compounds also suggests that these synthetic substances closely resemble the intended physiological function of the *qacA*−*qacR* locus. In contrast, unlike QacR, most MDR regulatory systems fail to increase the synthesis of their target genes in response to the known substrates of their cognate MDR transporters (*7*).

The versatile nature of the extended QacR ligand-binding pocket (*8*) is made more remarkable by the fact that structurally diverse compounds bind with submicromolar K_d values to each of the linked sites that make up the extended pocket: ethidium near the surface with a K_d of 0.81 ± 0.24 μM, rhodamine 6G in the more internal position with a K_d of 0.20 ± 0.02 μM, and the less-planar crystal violet in an intermediate location with a K_d of 0.3 ± 0.02 μM. Moreover, it is interesting to note that the K_d values determined for a number of QacR ligands were significantly lower than that of the most strongly bound ligand of the BmrR multidrug-binding protein (*43*). This suggests that the shared ability of these proteins to bind MDR substrates may be a closer match to the intended physiological function of QacR than it is to the natural function of BmrR. In summary, this study has provided additional evidence to support the notion that the primary function of the *qacA*−*qacR* system is to provide a general protection system against cationic and lipophilic toxic compounds, which includes a number of currently utilized antimicrobials, such as benzalkonium and chlorhexidine, antimicrobials that were historically employed as antiseptics, for example proflavin, and a range of natural plant antimicrobials. The lack of any clear-cut relationship between the structure of a QacR ligand and its K_d value indicates that the extended binding pocket has evolved to accommodate the broadest possible range of toxic hydrophobic cations, rather than a specific class of chemicals, endorsing a proposal that at least some MDR exporters function as general removal systems for hydrophobic molecules (*44*).

ACKNOWLEDGMENT

We are indebted to Dr. Ron Clarke, Dr. Adrienne Grant, and Dr. Warwick Payten for helpful discussions during the development of the tryptophan fluorescence assay and also to Dr. Monroe E. Wall and Dr. Mansukh C. Wanias for the supply of the compounds nitidine and avicin.

REFERENCES

1. Paulsen, I. T., Brown, M. H., and Skurray, R. A. (1996) *Microbiol. Rev. 60*, 575−608.
2. Kolaczkowska, A., and Goffeau, A. (1999) *Drug Resist. Updates 2*, 403−414.
3. Poole, K. (2001) *Curr. Opin. Microbiol. 4*, 500−508.
4. Gottesman, M. M., Pastan, I., and Ambudkar, S. V. (1996) *Curr. Opin. Genet. Devel. 6*, 610−617.
5. Yu, E. W., McDermott, G., Zgurskaya, H. I., Nikaido, H., and Koshland, D. E., Jr. (2003) *Science 300*, 976−980.
6. Grkovic, S., Brown, M. H., and Skurray, R. A. (2001) *Semin. Cell Dev. Biol. 12*, 225−237.
7. Grkovic, S., Brown, M. H., and Skurray, R. A. (2002) *Microbiol. Mol. Biol. Rev. 66*, 671−701.
8. Schumacher, M. A., Miller, M. C., Grkovic, S., Brown, M. H., Skurray, R. A., and Brennan, R. G. (2001) *Science 294*, 2158−2163.
9. Zheleznova Heldwein, E. E., and Brennan, R. G. (2001) *Nature 409*, 378−382.
10. Hsieh, P. C., Siegel, S. A., Rogers, B., Davis, D., and Lewis, K. (1998) *Proc. Natl. Acad. Sci. U.S.A. 95*, 6602−6606.
11. Lewis, K. (1999) *Curr. Biol. 9*, R403−R407.
12. Lewis, K. (2001) *J. Mol. Microbiol. Biotech. 3*, 247−254.
13. Nikaido, H., and Zgurskaya, H. I. (2001) *J. Mol. Microbiol. Biotechnol. 3*, 215−218.
14. Woolridge, D. P., Vázquez-Laslop, N., Markham, P. N., Chevalier, M. S., Gerner, E. W., and Neyfakh, A. A. (1997) *J. Biol. Chem. 272*, 8864−8866.
15. Markham, P. N., and Neyfakh, A. A. (2001) *Curr. Opin. Microbiol. 4*, 509−514.
16. Grkovic, S., Brown, M. H., Roberts, N. J., Paulsen, I. T., and Skurray, R. A. (1998) *J. Biol. Chem. 273*, 18665−18673.
17. Grkovic, S., Brown, M. H., Schumacher, M. A., Brennan, R. G., and Skurray, R. A. (2001) *J. Bacteriol. 183*, 7102−7109.
18. Schumacher, M. A., Miller, M. C., Grkovic, S., Brown, M. H., Skurray, R. A., and Brennan, R. G. (2002) *EMBO J. 21*, 1210−1218.
19. Tennent, J. M., Lyon, B. R., Midgley, M., Jones, I. G., Purewal, A. S., and Skurray, R. A. (1989) *J. Gen. Microbiol. 135*, 1−10.
20. Paulsen, I. T., Brown, M. H., and Skurray, R. A. (1998) *J. Bacteriol. 180*, 3477−3479.
21. Kuroda, M., Ohta, T., Uchiyama, I., Baba, T., Yuzawa, H., Kobayashi, I., Cui, L., Oguchi, A., Aoki, K., Nagai, Y., Lian, J., Ito, T., Kanamori, M., Matsumaru, H., Maruyama, A., Murakami, H., Hosoyama, A., Mizutani-Ui, Y., Takahashi, N. K., Sawano, T., Inoue, R., Kaito, C., Sekimizu, K., Hirakawa, H., Kuhara, S., Goto, S., Yabuzaki, J., Kanehisa, M., Yamashita, A., Oshima, K., Furuya, K., Yoshino, C., Shiba, T., Hattori, M., Ogasawara, N., Hayashi, H., and Hiramatsu, K. (2001) *Lancet 357*, 1225−1240.
22. Mitchell, B. A., Paulsen, I. T., Brown, M. H., and Skurray, R. A. (1999) *J. Biol. Chem. 274*, 3541−3548.
23. Mitchell, B. A., Brown, M. H., and Skurray, R. A. (1998) *Antimicrob. Agents Chemother. 42*, 475−477.
24. Brown, M. H., and Skurray, R. A. (2001) *J. Mol. Microbiol. Biotechnol. 3*, 163−170.
25. Galluzzi, L., Virtanen, P., and Karp, M. (2003) *Biochem. Biophys. Res. Commun. 301*, 24−30.
26. Sambrook, J., Fritsch, E. F., and Maniatis, T. (1989) *Molecular Cloning: A Laboratory Manual*, 2nd ed., Cold Spring Harbor Laboratory, Cold Spring Harbor, NY.
27. Kreiswirth, B. N., Lofdahl, S., Betley, M. J., O'Reilly, M., Schlievert, P. M., Bergdoll, M. S., and Novick, R. P. (1983) *Nature 305*, 709−712.
28. Kaatz, G. W., Seo, S. M., O'Brien, L., Wahiduzzaman, M., and Foster, T. J. (2000) *Antimicrob. Agents Chemother. 44*, 1404−1406.
29. Schenk, S., and Laddaga, R. A. (1992) *FEMS Microbiol. Lett. 73*, 133−138.
30. Lyon, B. R., May, J. W., and Skurray, R. A. (1983) *Antimicrob. Agents Chemother. 23*, 817−826.
31. McKenzie, T., Hoshino, T., Tanaka, T., and Sueoka, N. (1986) *Plasmid 15*, 93−104.
32. Bruckner, R. (1992) *Gene 122*, 187−192.

33. Tennent, J. M., Lyon, B. R., Gillespie, M. T., May, J. W., and Skurray, R. A. (1985) *Antimicrob. Agents Chemother. 27*, 79−83.
34. Ausubel, F. M., Brent, R., Kingston, R. E., Moore, D. D., Seidman, J. G., Smith, J. S., and Struhl, K. (1990) *Current Protocols in Molecular Biology*, John Wiley & Sons, New York.
35. Wu, J., Tisa, L. S., and Rosen, B. P. (1992) *J. Biol. Chem. 267*, 12570−12576.
36. Neyfakh, A. A., Borsch, C. M., and Kaatz, G. W. (1993) *Antimicrob. Agents Chemother. 37*, 128−129.
37. Kaatz, G. W., and Seo, S. M. (1995) *Antimicrob. Agents Chemother. 39*, 2650−2655.
38. Guay, G. G., and Rothstein, D. M. (1993) *Antimicrob. Agents Chemother. 37*, 191−198.
39. Darzynkiewicz, Z., Kapuscinski, J., Traganos, F., and Crissman, H. A. (1987) *Cytometry 8*, 138−145.
40. Paulsen, I. T., Brown, M. H., Littlejohn, T. G., Mitchell, B. A., and Skurray, R. A. (1996) *Proc. Natl. Acad. Sci. U.S.A. 93*, 3630−3635.
41. Grkovic, S., Brown, M. H., Hardie, K. M., Firth, N., and Skurray, R. A. (2003) *Microbiology 149*, 785−794.
42. Paulsen, I. T., Chen, J., Nelson, K. E., and Saier, M. H., Jr. (2001) *J. Mol. Microbiol. Biotechnol. 3*, 145−150.
43. Vázquez-Laslop, N., Markham, P. N., and Neyfakh, A. A. (1999) *Biochemistry 38*, 16925−16931.
44. Neyfakh, A. A. (2002) *Mol. Microbiol. 44*, 1123−1130.
45. Rouch, D. A., Cram, D. S., DiBerardino, D., Littlejohn, T. G., and Skurray, R. A. (1990) *Mol. Microbiol. 4*, 2051−2062.
46. Yanisch-Perron, C., Vieira, J., and Messing, J. (1985) *Gene 33*, 103−119.

BI035447+